DOI: 10.1534/genetics.104.031013

High-Resolution Fine Mapping and Fluorescence *in Situ* Hybridization Analysis of *sun*, a Locus Controlling Tomato Fruit Shape, Reveals a Region of the Tomato Genome Prone to DNA Rearrangements

E. van der Knaap,*,†,[1] A. Sanyal,‡ S. A. Jackson‡ and S. D. Tanksley†

**Department of Horticulture and Crop Science, Ohio State University/OARDC, Wooster, Ohio 44691, †Department of Plant Breeding and Department of Plant Biology, Cornell University, Ithaca, New York 14853 and ‡Department of Agronomy, Purdue University, West Lafayette, Indiana 47907*

Manuscript received May 8, 2004
Accepted for publication July 23, 2004

ABSTRACT

The locus *sun* on the short arm of tomato chromosome 7 controls morphology of the fruit. Alleles from wild relatives impart a round shape, while alleles from certain cultivated varieties impart an oval shape typical of roma-type tomatoes. We fine mapped the locus in two populations and investigated the genome organization of the region spanning and flanking *sun*. The first high-resolution genetic map of the *sun* locus was constructed using a nearly isogenic F_2 population derived from a cross between *Lycopersicon pennellii* introgression line IL7-4 and *L. esculentum* cv Sun1642. The mapping combined with results from pachytene FISH experiments demonstrated that the top of chromosome 7 is inverted in *L. pennellii* accession LA716. *sun* was located close to the chromosomal breakpoint and within the inversion, thereby precluding map-based cloning of the gene using this population. The fruit-shape locus was subsequently fine mapped in a population derived from a cross between *L. esculentum* Sun1642 and *L. pimpinellifolium* LA1589. Chromosome walking using clones identified from several large genomic insert libraries resulted in two noncontiguous contigs flanking *sun*. Fiber-FISH analysis showed that distance between the two contigs measured 68 kb in *L. esculentum* Sun1642 and 38 kb in *L. pimpinellifolium* LA1589, respectively. The *sun* locus mapped between the two contigs, suggesting that allelic variation at this locus may be due to an insertion/deletion event. The results demonstrate that *sun* is located in a highly dynamic region of the tomato genome.

FRUIT development commences with the development of carpel or gynoecium primordia within the floral meristem. The ovary, located at the base of the gynoecium, houses the ovules, which, after fertilization, promote the ovary to develop into a fruit. In recent years, molecular genetic approaches to dissect complex pathways of floral and fruit development have largely focused on a few model species. This research has resulted in a considerable increase in knowledge of plant development and the realization that genes and pathways regulating development have been largely conserved within the plant kingdom. However, relatively little focus has been placed on molecular processes underlying biological diversity. A greater understanding of the molecular nature underlying variation and diversity can provide additional insights into the regulation of biological processes.

Years of domestication and selection for its fruit characters have resulted in a substantial diversification of tomato fruit form. Quantitative genetic analyses have led to the identification of loci that control tomato fruit morphology (Grandillo *et al.* 1999). The subsequent cloning of genes underlying fruit morphology traits is of high importance, as those genes would reveal the molecular basis of tomato domestication, while also revealing the developmental pathways affected by alleles of these loci. Typically in tomato, successful map-based cloning experiments have relied on a set of introgression lines, each containing a segment of a distant wild relative of tomato, *L. pennellii* accession LA716, in an otherwise *Lycopersicon esculentum* background (Eshed and Zamir 1994). The level of nucleotide polymorphisms is sufficiently high between *L. esculentum* and *L. pennellii*, thus greatly expediting molecular marker development and hence map-based cloning of the gene of interest. These tomato introgression lines have been used extensively to clone genes underlying quantitative (Frary *et al.* 2000; Fridman *et al.* 2000) as well as qualitative (Pnueli *et al.* 1998; Isaacson *et al.* 2002) traits.

Chromosomal rearrangements occur during evolution and may involve major structural changes such as inversions and translocations as has been outlined in the grasses (Wilson *et al.* 1999). Between tomato and potato (*Solanum tuberosum*), there are thought to be five major inversions involving chromosomes 5, 9, 10, 11, and 12 (Tanksley *et al.* 1992). At least 28 rearrange-

[1]*Corresponding author:* Department of Horticulture and Crop Science, Ohio State University/OARDC, 1680 Madison Ave., Wooster, OH 44691. E-mail: vanderknaap.1@osu.edu

ments differentiate the tomato and eggplant (*S. melongena*) genomes (Doganlar *et al.* 2002). Even more chromosomal rearrangements are reported between the more distant Solanaceous genera Lycopersicon and Capsicum, including extensive gene duplication (Livingstone *et al.* 1999). However, within the genus Lycopersicon, few major chromosomal rearrangements have been reported to date.

This study was undertaken to fine map *sun*, a locus controlling tomato fruit shape from a round to an oval shape typical of roma-type tomatoes (van der Knaap and Tanksley 2001). *sun* maps near marker CT52 on the middle of the short arm of chromosome 7 and is the only major locus identified in the population derived from a cross between *L. esculentum* Sun1642 and *L. pimpinellifolium* LA1589, a close wild relative of cultivated tomato. The phenotypic variance explained by CT52 is 58%, and the LOD score is nearly 18 (van der Knaap and Tanksley 2001). Progeny tests of recombinant F_2 plants in the interval LED21J7 and T42 placed *sun* precisely to the 6-cM interval between TG576 and GP121 (Figure 2A). Results from the current study demonstrated the location of *sun* to a 38- to 68-kb region of the short arm of chromosome 7. *sun* was located near an inversion breakpoint in a wild relative of tomato, *L. pennellii* accession LA716. Furthermore, the locus itself underwent an insertion/deletion event of ~30 kb, which may be the cause of allelic variation at *sun*. The powerful combination of genome structure analysis and high-resolution fine mapping demonstrated that *sun* is located in a highly dynamic region of the tomato genome.

MATERIALS AND METHODS

Plant material: Populations derived from a single cross between inbred lines *L. pimpinellifolium* accession LA1589 and *L. esculentum* cv Sun1642 are hereafter denoted as EPM (Figure 1). The nearly isogenic F_2 population derived from a cross between Sun1642 and IL7-4, an *L. esculentum* line, which harbors a segment of chromosome 7 from *L. pennellii* accession LA716 (Eshed and Zamir 1994) is hereafter denoted as EPN. Recombinants identified from the EPN population were grown in greenhouses of the Boyce Thompson Institute on the Cornell University campus (Figure 1).

For the second high-resolution recombinant screen, 18 F_2 EPM plants, heterozygous for the interval CD57-TG342 (short arm of chromosome 7) were selected. Seventy-two seeds from each heterozygous F_2 plant were sown to select recombinants from these F_3 families. One additional line, 00T281, obtained while backcrossing the Sun1642 allele of *sun* in the LA1589 background, showed high levels of recombination in its BC_2 progeny. Selfed 00T281 seed, constituting the 19th family, were germinated and screened for additional recombinants (Figure 1). Testing of F_4 progeny of F_3 recombinants was performed in the greenhouse or in the field at the Ohio Agricultural Research and Development Center (OARDC, Wooster, OH).

High-resolution recombinant screens: DNA from plants of the EPN population was isolated by placing leaves from seedlings in flat-bottom, 96-well microtiter plates. After addition of DNA extraction buffer (Fulton *et al.* 1995), tissues were ground with a 96-pestle (HyPure, Wallac, Norton, OH) and incubated at 65° for 20 min. Extraction buffer containing DNA was transferred to a round-bottom microtiter plate. DNA was precipitated by adding 2× volume of ethanol/0.2 M NaOAc, pH 7, to the samples followed by centrifugation at 3400 × *g*. The supernatant was poured off and pellets were allowed to dry at room temperature. Pellets were resuspended in 100 μl TE, and 3 μl of resuspended DNA was used for each PCR reaction. CT52 and TG576 were converted to codominant PCR-based markers as described previously for cleaved amplified polymorphic sequences (CAPS; Konieczny and Ausubel 1993; Table 1).

DNA from plants of the EPM population was isolated using the microprep method (Fulton *et al.* 1995) and digested with *Sca*I. Digested DNA was subjected to DNA gel-blot analysis as previously described (Bernatzky and Tanksley 1986). The blots were sequentially hybridized to GP121 and Le76E24-U probes to identify plants with a recombination breakpoint between these two markers.

Large genomic insert isolation: Genomic clones spanning *sun* were identified from three large insert libraries. All *L. esculentum* clones were identified from a Heinz 1706 library constructed with a pBeloBAC11 vector (Budiman *et al.* 2000). These clones are denoted as Le followed by the address of the clone in the library. All other clones contained *L. pennellii* accession LA716 genomic DNA, and the clones are denoted as Lp followed by the address of the clone in the library. The *L. pennellii* clones were from a library constructed with the cosmid vector pCLD04541 (accession no. AF184978), except Lp12L2 clone, which was identified from a library with pBeloBAC11 as vector. Both *L. pennellii* libraries were kindly provided by J. J. Giovannoni, U.S. Department of Agriculture Plant, Soil, and Nutrition Research Laboratory (Ithaca, NY). Sequential hybridization of the following probes to the library filters were done as described for DNA gel-blot analysis and resulted in identification of the following clones: TG576 resulted in identification of clone Le76E24; LPT4D21 resulted in identification of clones Lp81B9, Lp103E7, Lp104D16, Le27J5, Le37F23, Le124E22, Le236C15, and Le278H2; Lp81B9-FF and Lp103E7-R resulted in identification of clones Le33O1, Lp12L2, and Lp61O2.

End-clone sequences and probes: DNA fragments of the ends of clones Le27J5, Le76E24, Le124E22, Le236C15, and Le278H2 were obtained by *Nsi*I digestion of BAC DNA, followed by transformation of the self-ligated product in *Escherichia coli* using standard molecular biology techniques (Sambrook *et al.* 1989). The pBeloBAC11 vector does not contain *Nsi*I sites, thus allowing subcloning of BAC ends. Remaining inserts <3 kb were amplified with the M13F and M13R primers, digested with *Nsi*I, and run on agarose gel to isolate each end separately. Of the two fragments obtained, the larger DNA fragment is called U (upper) and the smaller fragment is called L (lower). For inserts too large to be amplified, end fragments were isolated after *Hin*dIII (the cloning site of inserts) and *Nsi*I digestion of the plasmid and separation on agarose gel. *Nsi*I digestion and self-ligation of the cosmid clone Lp103E7 allowed subcloning of only the M13F end of this clone. Insert from the subcloned Lp103E7 clone was isolated from agarose gel following plasmid digestion with *Hin*dIII and *Nsi*I. These fragments were used for DNA gel-blot analysis and denoted as the clone name with the "U" or "L" extension (*i.e.*, Le124E22-U).

The end sequences of clones Le33O1, Le37F23, Lp12L2, Lp61O2, Lp81B9, Lp103E7, and Lp104D16 were obtained by direct sequencing of the large insert clones [Amplicon Express (Pullman, WA) and the Cornell DNA Sequencing Facility], using the M13F and M13R primers. The end fragments were

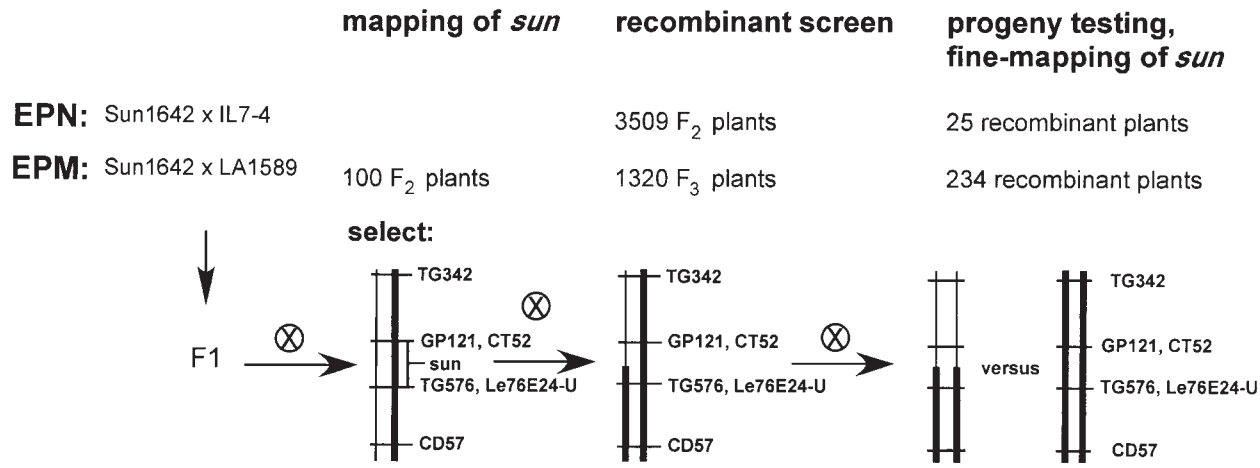

FIGURE 1.—Diagram of the populations used to fine map *sun*. EPN, population derived from a cross between nearly isogenic *L. esculentum* Sun1642 and IL7-4. EPM, population derived from a cross between *L. esculentum* Sun1642 and *L. pimpinellifolium* LA1589. Thin and thick lines represent alleles of either parent. Two thick or thin lines represent homozygosity at that locus, while a thick and a thin line represent heterozygosity at the locus. Circled ×'s indicate selfing of the plant. *sun* was initially mapped in a population of 100 F_2 plants. For high-resolution fine mapping, recombinant screens were conducted in 3509 and 1320 seedlings of the EPN and EPM population, respectively. The recombinants thus identified were progeny tested and phenotypically analyzed to verify the precise location of *sun*.

denoted as F and R, respectively (*i.e.*, Le33O1-F). Locus-specific primers were designed to amplify each end from genomic DNA and the resulting fragments were used as template to generate radioactively labeled probe for DNA gel-blot analysis or sequenced to identify nucleotide polymorphisms between the parents for PCR-based mapping. Fragments >350 bp were labeled using the random primer labeling method (FEINBERG and VOGELSTEIN 1983). Fragments <350 bp were labeled by a three-cycle amplification step (94° for 1 min, 50° for 10 min, 72° for 1 min) in 10 mM Tris-Hcl, pH 8.3, 50 mM KCl, 3 mM MgCl2, 75 μM of each dATP, dGTP and dTTP, 25 μCi of [α-^{32}P] dCTP (3000 μCi /μmol), 50 ng of template DNA, 125 nM of each primer, and 1 unit of *Taq* polymerase in a total volume of 25 μl.

Mapping of ends of large genomic insert clones: Most end fragments were mapped in the recombinant population as RFLP markers (Table 1). End fragments in the near vicinity of *sun* were mapped as single nucleotide polymorphism (SNP) or as insertion or deletion (indels). The three SNPs between the alleles of marker Lp81B9-F were scored by using dHPLC (UNDERHILL *et al.* 1997) at the Institute for Genomic Diversity, Cornell University (Ithaca, NY). In addition, the map position of Lp81B9-F was confirmed by RFLP analysis. Markers Lp103E7-R, Le33O1-F, and Le37F23-R showed indels between alleles amplified from Sun1642 and LA1589 parents (Table 1). Amplified Lp103E7-R, Le33O1-F, and Le37F23-R fragments from DNA isolated from recombinant plants were separated, visualized, and scored on a Perkin-Elmer (Norwalk, CT) ABI377 at the Molecular and Cellular Imaging Center, OARDC (Wooster, OH). Le33O1-R was mapped as a SNP by sequencing the alleles amplified from DNA of recombinant plants in the interval Lp81B9-F and Lp61O2-F. The dominant marker Lp61O2-R (61R1 and 61R2 primers fail to amplify the LA1589 allele) was scored for the presence or absence of an amplification product in the F_4 progeny, thus allowing reconstitution of the Lp61O2-R genotype in the F_3 recombinant plant.

Fluorescence *in situ* hybridization analysis: For fiber fluorescence *in situ* hybridization (FISH) analysis, nuclei were isolated from young leaf tissue taken from greenhouse-grown Sun1642 and LA1589 plants following previously published procedures (ZHONG *et al.* 1996), except that 22-μm nylon mesh was used for the last filtration. The extended DNA fibers were prepared on poly-L-lysine (Sigma, St. Louis) microscope slides following previously detailed protocols (JACKSON *et al.* 1998). Pachytene chromosomes were prepared from anthers fixed in 3:1 ethanol to glacial acetic acid. To extrude the meiocytes, the anthers were nicked at the end. The meiocytes were squashed in 45% acetic acid, and the integrity of the chromosomes was checked with a phase-contrast microscope.

To label probes, 1 μg of plasmid DNA was used for nick translation incorporating either biotin-UTP or digoxigenin-UTP. FISH was done following previously published protocols (JIANG *et al.* 1996). Briefly, probe was added to the slides, a coverslip was mounted and sealed with rubber cement, and the slides were incubated at 37° in a humid environment overnight. Biotin-labeled probes were detected using AlexaFluor 488 strepavidin (Molecular Probes, Eugene, OR) and digoxigenin-labeled probes were detected using mouse antidigoxigenin followed by AlexaFluor 568 anti-mouse (Molecular Probes). Coverslips were mounted in VectaShield (Vector Labs, Burlingame, CA). Slides were analyzed and digital images captured using either an Olympus BX60 with a Hamimatsu Orca ER CCD camera controlled with MetaMorph (Universal Imaging, West Chester, PA) or a Nikon E400 with an Optronics MagnaFire CCD camera controlled by ImagePro (Media Cybernetics). Images were further analyzed using MetaMorph and final publication images were prepared using Adobe Photoshop v7.0 for Macintosh. To calculate the insert size of each clone and the physical distance between the contigs, at least 20 measurements were taken. The bracketed number preceding the physical size indicates standard deviation. The significance of differences in physical length were determined by Student's *t*-test.

Genetic distance and phenotypic and statistical analyses: The genetic distance between markers in centimorgans was calculated as the number of recombinants between two markers divided by the number of gametes screened, multiplied by 100. Using marker-assisted selection, at least four homozygous recombinant and four homozygous nonrecombinant seedlings were identified in each of two EPN single recombinant-derived F_3 families (Table 2) and in 27 of the EPM single

TABLE 1

Markers used in the high-resolution fine mapping of *sun*

Marker name	Size	Origin	Copy number	Primers	Use
TG576	1.3 kb	Genomic clone, tomato map (Pillen *et al.* 1996)	1	TG576-R1: AAGGTCAAATGGCAGTCACC TG576-F2: CCGAAACGGGGAAAAATAAT	CAPS marker in EPN/SNP in EPM
CT52	1.2 kb	cDNA clone, tomato map (Pillen *et al.* 1996)	1	CT52-F2: GGCAAAATCAAGATCCAAGC CT52-R4: GGTTTGTGGGAGAGATGAGG	CAPS marker in EPN/RFLP marker in EPM
GP121	0.95 kb	Genomic clone potato map (Gebhardt *et al.* 1991)	1		RFLP marker in EPM
cLPT4D21	1.2 kb	Tomato EST	1		RFLP marker in EPM
Le33O1-R	306 bp	PCR product from Le33O1, M13R end	1	33R1: CATGAGAGGAGACCCCTTTTT 33R2: GGGTTGCATCTCATTTGTCA	RFLP and SNP in EPM
Le33O1-F	278 bp	PCR product from Le33O1, M13F end	Multiple copy	33F1: CAAATCTCACATCGAAAAGACA 33F3: TTGTATATCAAATCAGATGGCAAAA	SNP and indel in EPM
Le37F23-F	397 bp	PCR product from Le37F23, M13F end	1	37F1: ACAAGGTGCCAACAACACTG 37F2: GCCAGAACGAAGCAGCTTTA	RFLP marker in EPN
Le37F23-R	287 bp	PCR product from Le37F23, M13R end	2–3	37R3: TTTCTCCTTGCCAAGTCTGG 37R4: TGGTATGGCTGCCCTAAGAC	Indel in EPM
Le76E24-U	2.9 kb	*Nsi*I-digested subclone of Le76E24, large fragment	1		RFLP marker in EPM
Le76E24-L	0.6 kb	*Nsi*I-digested subclone of Le76E24, small fragment	1		RFLP marker in EPM
Le124E22-U	1.6 kb	*Nsi*I-digested subclone of Le124E22, large fragment Identical to Le278H2-U	1		RFLP marker in EPM and EPN
Le236C15-U	1.2 kb	*Nsi*I-digested subclone of Le236C15, large fragment. Identical to Le278H2-L, Le27J5-L	1		RFLP marker in EPM
Le236C15-UU	400 bp	PCR product from Le236C15, M13R end	1	236R1: TCGACGTGGTGAAGAGTCAA 236R2: TGTTTGGGTTGTTTGGTGAA	SNP in EPM
Le236C15-L	0.6 kb	*Nsi*I-digested subclone of Le236C15, small fragment	1		RFLP marker in EPN
Lp12L2-F	306 bp	PCR product from Lp12L2, M13F end	1	12F1: ACCGATTCCTCAAGTTCAGC 12F2: TTCCAAGACCAAGAGCATCC	RFLP marker in EPM
Lp61O2-F	297 bp	PCR product from Lp61O2, M13F end	1	61F1: CATCCTCGTTCGGCTGTAAT 61F2: ACCCCATCTTCACTGACTCC	RFLP marker in EPM
Lp61O2-R	298 bp	PCR product from Lp61O2, M13R end	Multiple copy	61R1: TGCATCAACTAGCTGACCCTTA 61R2: TCGTCATATTGCGCTTATCG	Dominant marker in EPM
Lp81B9-F	290 bp	PCR product from Lp81B9, M13F end	Smear	81F1: GCTTGCTATTGGGACCTTCA 81F2: CCCATAACCTCCTCGTTTGA	SNP in EPM, temperature for dHPLC is 55°
Lp81B9-FF	473 bp	PCR product from Lp81B9, probe for library screen. Amplifies only *L. pennellii* allele	2	81R3: TTTCCAGGGGCATTTATTGA 81R4: AAGCCATGATTAATACACAAAAAGC	RFLP marker in EPM
Lp103E7-F	1 kb	*Nsi*I-digested subclone of Lp103E7, HIII fragment			RFLP marker in EPM
Lp103E7-R	275 bp	PCR product from Lp103E7, M13R end	2	103R1: GGGGAAGGTCCATCACAGTA 103R2: TTCCTAAGGTTCATTAATCCAAAA	RFLP marker and indel in EPM
Lp104D16-F	287 bp	PCR product from Lp104D16, M13F end	1	104F1: GCTTCATCGAAATGTGAGATGT 104F3: CAAAATTCCAACATAAATGACGAA	RFLP marker in EPM
TGR1	162 bp	Subtelomeric repeat (Schweizer *et al.* 1988)	Multiple copy	EP65: CCAACCGTATGCATAGACAA EP66: CGTTTGGAAGGTCAAACGAG	NA

CAPS, cleaved amplified polymorphic sequence; EPM, *esculentum-pimpinellifolium* population; EPN, *esculentum-pennellii* population.

TABLE 2

Phenotypic analysis of progeny of *sun* locus recombinants of the EPN population

Recombinant F_2 parent	Marker					Average fruit-shape index of progeny[a]		
	TG576	Le76E24-U	Le37F23-F	Le236C15-L	LPT4D21/Le236C15-U /GP121/CT52/sun	Recombinant	Nonrecombinant	P^b
00T869B-816	3	3	3	3	2	1.49	0.93	***
00T869C-279	2	2	2	2	3	0.96	0.93	NS

A score of 2 indicates heterozygous; 3 indicates homozygous LA716.

[a] Fruit shape is measured as the average ratio of length to diameter of fruit in the recombinant and nonrecombinant class, respectively.

[b] Significance of Student's *t*-test: ***, $P < 0.001$; NS, not significant. Only parents heterozygous for *sun* show significant differences in progeny tests for genotypic classes.

recombinant-derived F_4 families (Figure 1, Table 3). Mean fruit-shape index (measured as the ratio of length to diameter of the fruit) of plants in the recombinant class was contrasted to shape index of the nonrecombinant class in each family using Student's *t*-test at $P < 0.01$ (van der Knaap and Tanksley 2001).

RESULTS

Previously, we mapped the fruit-shape locus *sun* between marker CT52 and LED21J7 on the short arm of tomato chromosome 7 (van der Knaap and Tanksley 2001). We placed additional markers on the linkage map constructed with the original population of 100 F_2 plants that identified *sun* (Figure 2A). Markers TG576 and GP121 clearly flank *sun* as is demonstrated by the occurrence of several recombinants between these markers and the locus.

High-resolution fine mapping of *sun* in the EPN population: To reduce the effect of minor loci confounding phenotypic analysis and increase the level of nucleotide polymorphisms for efficient marker development, a high-resolution genetic map of the *sun* locus was constructed using a nearly isogenic F_2 population derived from a cross between Sun1642 and IL7-4, an *L. esculentum* line, which harbors a segment of chromosome 7 from *L. pennellii* accession LA716. A total of 3509 F_2 seedlings screened for recombination events between markers TG576 and CT52 resulted in the identification of 25 recombinants in this interval (Figure 1, Figure 2B).

Identification of large genomic insert clones near sun: The marker most closely linked to *sun*, LPT4D21, was used to screen *L. esculentum* and *L. pennellii* large genomic insert libraries and resulted in the identification of eight clones. Inserts of these eight clones were aligned relative to each other by DNA gel-blot analysis with end probes of each insert, and PCR analysis using primers derived from the end sequences (bottom of Figure 2C, LPT4D21 contig). Despite hybridization of clone ends in the direction proximal to *sun*, no hybridization of *L. pennellii* and *L. esculentum* clone ends distal to *sun* were detected (Figure 2C). For example, Le27J5-U hybridized to all *L. esculentum* clones and not to any of the *L. pennellii* clones. Equally, Lp103E7-F hybridized to the three *L. pennellii* clones and not to any of the *L. esculentum* clones.

Mapping of sun and end markers: To further delineate the map position of *sun*, we placed the large insert end fragments as markers onto the high-resolution genetic map. As shown in Figure 2B, the end markers Le236C15-L and Le124E22-U mapped 0.03 and 0.12 cM from CT52, respectively, and Le76E24-U mapped 0.03 cM from TG576 in the EPN population. However, end markers Le236C15-U and Lp103E7-R cosegregated with CT52, as did markers LPT4D21 and GP121 (Figure 2B). These results indicated that recombination appeared evenly distributed in the TG576-LPT4D21 interval, albeit occurring at low frequencies, while no recombination event occurred in the LPT4D21-CT52 interval. The fruit-shape locus *sun* was also mapped in the high-resolution recombinant EPN population. F_3 families derived from the two F_2 plants that are recombinant in the interval Le236C15-L-CT52 were analyzed for variation in fruit shape within each family. Fruit-shape index was calculated as the ratio of the length to the width of the fruit. Significant differences in fruit-shape index between the recombinant and nonrecombinant class within each family indicated that the F_3 family consisted of plants producing either round or elongated fruit, and the genotype of *sun* was heterozygous in the recombinant F_2 plant. On the other hand, similar fruit-shape indices between recombinant and nonrecombinant classes indicate homozygosity at the *sun* locus. Phenotypic analysis of fruit shape in the progeny of these two recombinant EPN plants clearly demonstrated that *sun* cosegregated with LPT4D21, GP121, and CT52 (Table 2). The lack of recombination events delineating the *sun* locus in the EPN population precludes the identification of the gene encoded by *sun* using this population.

To investigate the potential cause of the drop in recombination frequency in the interval LPT4D21-CT52, the end fragments of *L. pennellii* clone Lp103E7 were mapped in the EPM population (Figure 2A). As indicated above, the Lp103E7 end fragment distal to *sun*, Lp103E7-F, did not overlap with any of the *L. esculentum* large insert clones, and vice versa. The mapping results

TABLE 3

Phenotypic analysis of progeny of *sun* locus recombinants of the EPM population

Recombinant F_3 parent	Marker										Average fruit-shape index of progeny[a]		
	Le124E22-U	Le236C15-U	Lp103E7-R	Lp81B9-F	sun	Lp61O2-R	Le33O1-R	Lp61O2-F	Le33O1-F	Lp12L2-F	Recombinant	Nonrecombinant	P^b
00T1316-31	*2*	*3*	3	3	3	3	3	3	3	3	0.95	0.92	NS
00T1316-83	*2*	*3*	3	3	3	3	3	3	3	3	0.98	0.94	NS
00T1316-35	1	*1*	*2*	2	2	2	2	2	2	2	0.94	1.56	**
01T8-62	2	2	*2*	*3*	3	3	3	3	3	3	0.92	0.92	NS
01T19-52	2	2	*2*	*3*	3	3	3	3	3	3	0.98	0.98	NS
01T19-65	3	3	*3*	*2*	2	2	2	2	2	3	1.66	0.97	****
01T41-56	1	1	*1*	*2*	2	2	2	2	2	2	1.05	1.92	***
01T8-50	2	2	2	*2*	*3*	*3*	3	3	3	3	0.84	0.87	NS
01T19-24	1	1	1	*1*	*1*	*2*	2	2	2	2	1.21	1.3	NS
01T37-70	2	2	2	*2*	*3*	*3*	3	3	3	3	0.8	0.79	NS
01T39-27	2	2	2	*2*	*2*	*1*	1	1	1	1	0.83	1.23	**
01T19-27	3	3	3	3	3	*3*	*2*	2	2	2	0.98	0.96	NS
01T36-18	2	2	2	2	2	*2*	*3*	3	3	3	1.59	1	****
01T40-66	2	2	2	2	2	*2*	*1*	1	1	1	0.96	1.99	***
01T8-68	3	3	3	3	3	*3*	*3*	*2*	2	2	1.06	1	NS
01T10-9	2	2	2	2	2	2	*2*	*3*	3	3	1.55	0.87	***
01T12-9	3	3	3	3	3	3	*3*	*2*	2	2	0.94	0.93	NS
01T12-13	1	1	1	1	1	1	*1*	*2*	2	2	1.33	1.47	NS
01T12-55	3	3	3	3	3	3	*3*	*2*	2	2	0.98	0.98	NS
01T20-33	2	2	2	2	2	2	*2*	*3*	3	3	1.52	0.96	**
01T21-4	3	3	3	3	3	3	*3*	*2*	2	2	1.07	1.05	NS
01T7-69	1	1	1	1	1	1	1	*1*	*2*	2	1.18	1.15	NS
01T9-53	2	2	2	2	2	2	2	*2*	*3*	3	1.25	0.91	**
01T11-41	3	3	3	3	3	3	3	*3*	*2*	2	1.22	1.2	NS
01T40-49	1	1	1	1	1	1	1	*1*	*2*	2	1.76	1.7	NS
01T20-32	2	2	2	2	2	2	2	2	*2*	*3*	1.58	1.01	**
01T38-44	2	2	2	2	2	2	2	2	*2*	*3*	1.6	0.99	**

Interval in which the recombination event occurred is italic. Markers were derived from BAC ends that mapped near *sun* (Figure 2). A score of 1 indicates Sun1642; 2 indicates heterozygous; 3 indicates LA1589. Recombinant interval surrounding the *sun* locus is underlined.

[a] Fruit shape is measured as the average ratio of length to diameter of fruit in the recombinant and nonrecombinant class, respectively.

[b] Significance of Student's *t*-test: **, $P < 0.01$; ***, $P < 0.001$; ****, $P < 0.0001$; NS, not significant. Only parents heterozygous for *sun* show significant differences in progeny tests.

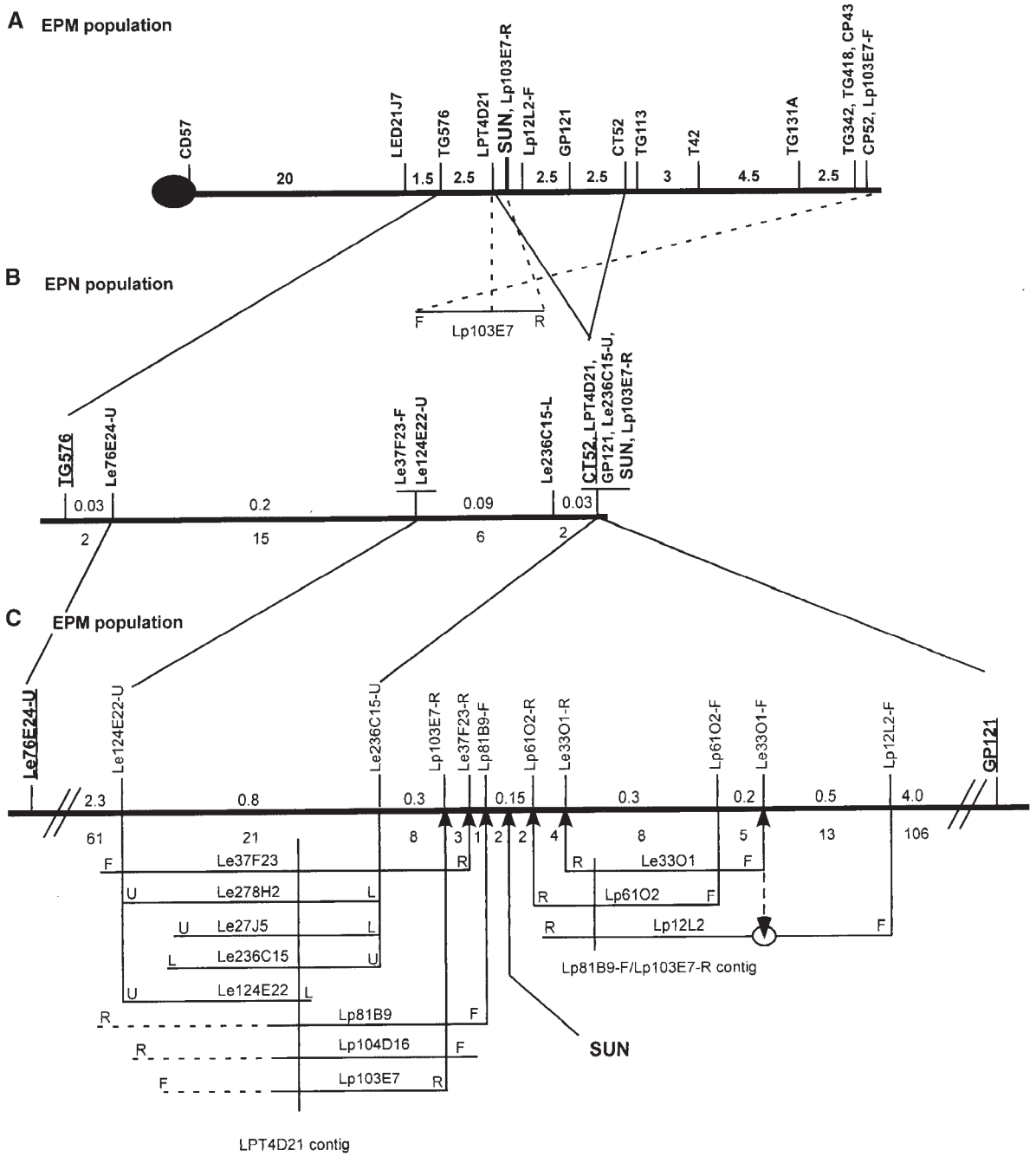

FIGURE 2.—Genetic map of the *sun* locus. (A) Low-resolution map position of *sun* and markers on the short arm of chromosome 7 inferred from the EPM population. Solid circle on the left of the chromosome denotes the centromere. The telomere is located on the right. Numbers above the line indicate centimorgan distance between markers. (B) High-resolution genetic map of *sun* locus inferred from the EPN population. Number above the chromosome indicates centimorgan distance between markers; number below the chromosome indicates number of recombinant plants identified in the respective interval. Markers used for high-resolution recombinant screening are underlined. (C) High-resolution genetic map of *sun* locus inferred from the EPM population. Thick horizontal line indicates the chromosome; thin lines below the chromosome indicate genomic large insert clones. Vertical lines from the large insert ends to the chromosome indicate the genetic position of these ends as RFLP markers on the high-resolution map. Arrows from the large insert ends to the chromosome indicate the genetic position of these ends as SNP or indel markers. Numbers above the chromosome indicates centimorgan distance between markers; numbers below the chromosome indicates number of recombinant plants identified in the respective interval. Connectors among Le278H2-L, Le236C15-U, and Le27J5-L, for example, indicate identical ends of large insert clones.

demonstrated that while Lp103E7-R cosegregated with *sun*, Lp103E7-F mapped to the top of chromosome 7, 16 cM away from *sun* (Figure 2A). Therefore, the sudden drop in recombination frequency in the interval LPT-4D21-CT52, combined with the large genetic distance between the ends of *L. pennellii* clone Lp103E7 in the EPM population (Figure 2, A and B), suggested the presence of a paracentric inversion in the *L. pennellii* genome compared to the LA1589 and Sun1642 genomes.

FISH analysis of the *sun* locus: To further investigate the inversion of the top part of chromosome 7 in *L. pennellii* LA716, we conducted pachytene FISH with clones Le37F23 and Le33O1 as probe (Figure 3, A–C). These clones map partly and entirely within the inversion, respectively (Figure 2, B and C). As shown in Figure 3A, results from the FISH analysis demonstrated that clones Le37F23 and Le33O1 colocalized to the telomere of chromosome 7 in *L. pennellii* LA716, while the same clones colocalized well below the telomere and to the euchromatic region of chromosome 7 in *L. esculentum* Sun1642 and *L. pimpinellifolium* LA1589 (Figure 3, B and C, respectively). The FISH results were consistent with results from the genetic experiments, which suggested that the large genetic distance between the ends of *L. pennellii* clone Lp103E7 in the EPM population and the complete absence of recombination in the interval LPT4D21-CT52 in the EPN population was due to a paracentric inversion in *L. pennellii* accession LA716 compared to the Sun1642 and LA1589 genomes. We also hybridized the *L. pennellii* clones Lp103E7 and Lp81B9, which span the inversion breakpoint, to *L. pennellii* pachytene chromosomes. The hybridization signal of these probes colocalized to the telomeric ends of *L. pennellii* chromosomes (Figure 3D). Tomato telomeres consist of a telomeric repeat (TR) at the very end of the chromosome followed by a subtelomeric repeat (TGR1), and each chromosome end displays an organization pattern of TR and TGR1 unique to that chromosome (Zhong *et al.* 1998). As shown in Figure 3E, FISH analysis of extended DNA fibers using Lp81B9 as probe revealed a hybridization pattern strikingly similar to that observed with TGR1 as probe (Zhong *et al.* 1998). To examine whether the subtelomeric repeat TGR1 is present on clones Lp81B9 and Lp103E7, we conducted PCR analysis using TGR1-specific primers as well as Southern blot analysis. PCR analysis showed that the *L. pennellii* clones Lp81B9 and Lp103E7, which span the breakpoint and show pachytene FISH localization at the telomeric end of tomato chromosomes, contain the subtelomeric repeat TGR1, while the *L. esculentum* clones Le37F23 and Le236C15 lack the TGR1 repeat (Figure 3F). TGR1 was hybridized as probe to blots containing *Eco*RV-digested large insert DNA of the clones shown in Figure 2C, and identical results were obtained: the TGR1 probe hybridized to a high molecular weight fragment present in *L. pennellii* clones Lp81B9, Lp103E7, and Lp104D16, and not to any of the other clones (data not shown). These results support the notion of the telomeric origin of *L. pennellii* clones Lp81B9 and Lp103E7 as these clones harbor the subtelomere-specific sequence TGR1.

High-resolution fine mapping of *sun* in the EPM population: Due to the lack of recombination events delineating the *sun* locus, fine mapping of *sun* in the EPN population was unsuccessful. We then proceeded to fine map *sun* in the EPM population. To reduce the confounding effect of minor segregating loci, a high-resolution genetic map of the *sun* locus was constructed using a large F_3 population derived from F_2 plants heterozygous for the entire short arm of chromosome 7. A total of 1320 EPM plants were screened, resulting in 234 recombinants between markers Le76E24-U and GP121 (Figures 1 and 2C).

Construction of a contig of the sun locus: The physical map was extended farther by using DNA fragments Lp81B9-FF and Lp103E7-R as probes to screen large genomic insert libraries for additional clones. Hybridization with Lp81B9-FF and Lp103E7-R probes resulted in the identification of one *L. esculentum* and two *L. pennellii* clones (Figure 2C). The clones were aligned relative to each other via DNA gel-blot analysis with the end probes and PCR analysis using primers derived from the end sequences. Mapping of the ends showed that the most distal fragment, Lp12L2-F, mapped one recombination event distal to and past *sun* in the original F_2 population (Figure 2A). These results suggested that the identified large genomic insert clones spanned the fruit-shape locus *sun*. However, despite hybridization of Lp81B9-FF and Lp103E7-R probes to DNA from the three new clones, no hybridization was observed of

Figure 3.—FISH analysis of the *sun* locus. The chromosomes are colored in blue (A) Mitotic chomosomes of *L. pennellii* LA716. The fluorescently labeled probes Le37F23 (green) and Le33O1 (red) colocalize to the tip of LA716 chromosome 7. Bar, 5 μm. (B) Meiotic chromosomes of *L. esculentum* Sun1642. The fluorescently labeled probes Le37F23 (green) and Le33O1 (red) colocalize (arrow) well below the telomere (arrowhead). Note the intense blue staining of the telomeric end indicative of heterochromatin. (C) Meiotic chromosomes of *L. pimpinellifolium* LA1589. The fluorescently labeled probes Le37F23 (green) and Le33O1 (red) colocalize (arrow) well below the telomere (arrowhead). (D) Mitotic chromosomes of *L. pennellii* LA716. The bright staining of the colocalized fluorescently labeled probes Lp81B9 and Lp103E7 map to the tips of many chromosomes. (E) Fluorescently labeled Lp81B9 probe hybridized to *L. esculentum* Sun1642 chromatin fibers. Note the repetitive hybridization signal. (F) PCR and agarose gel analysis indicating the presence or absence of the subtelomeric repeat TGR1 on the large insert clones indicated above the lanes. The numbers on the left of the gel indicate the molecular weight in base pairs. The lower band shows the expected size of the repeat (162 bp) while the upper band appears to be a TGR1 doublet (~320 bp).

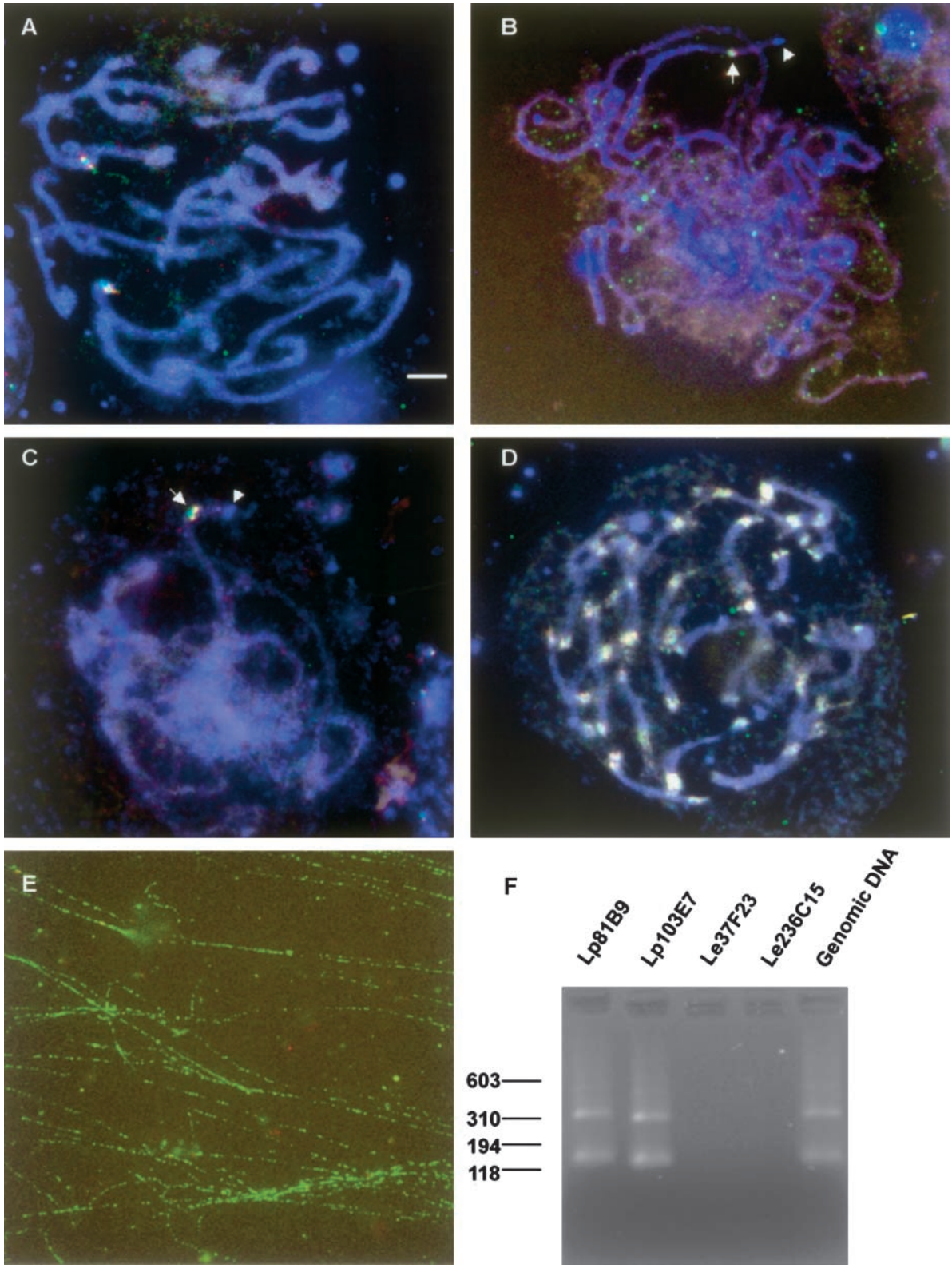
A
B
C
D
E
F
Lp81B9
Lp103E7
Le37F23
Le236C15
Genomic DNA
603
310
194
118

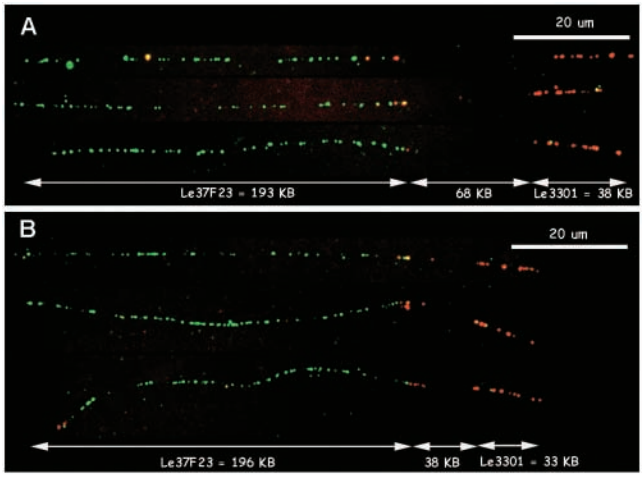

FIGURE 4.—Fiber FISH analysis of the *sun* locus. (A) Fluorescently labeled probes derived from clones Le37F23 (green) and Le33O1 (red) were hybridized to *L. esculentum* Sun1642 chromatin fibers. Three representative images are shown and the average size of the clones and the gap are indicated below the probe signals. (B) Fluorescently labeled probes derived from clones Le37F23 (green) and Le33O1 (red) were hybridized to *L. pimpinellifolium* LA1589 chromatin fibers. Three representative images are shown and the average size of the clones and the gap are indicated below the probe signals. (A and B) Bar, 20 μm; the conversion is 2.9 kb/μm.

Lp61O2-R, Lp12L2-R, and Le33O1-R probes to DNA from clones in the first contig. These results indicated the presence of a gap in the contig. The alignment of the genomic inserts, the orientation of the contig relative to *sun*, and the presence of the gap were confirmed by mapping the ends of the large insert clones onto the high-resolution map of the EPM population (Figure 2C).

Fine mapping of sun: The precise genomic location of *sun* was determined by progeny testing of F_3 EPM recombinant plants that map to contiguous intervals near *sun* (Table 3). F_4 families derived from individual F_3 recombinants were analyzed for variation in fruit shape within each family. Fruit-shape indices for plants homozygous for the Sun1642 allele at *sun* (scored as 1 in Table 3) ranged from 1.15 to 1.99 with an average index of 1.5. Fruit-shape indices for plants homozygous for the LA1589 allele at *sun* (scored as 3 in Table 3) ranged from 0.79 to 1.22 with an average index of 0.97. The small but notable overlap in fruit-shape indices suggests the existence of other minor loci present in this population and/or environmental effects on the degree of fruit elongation. Progeny testing clearly demonstrated that *sun* was located in the interval Lp81B9-F and Lp61O2-R, two recombination events from either marker. Unfortunately, clones containing this region of the genome are absent from the genomic libraries that were screened (Figure 2C and Table 3).

Genome structure analysis of the *sun* locus: To determine the physical distance between the two contigs flanking the *sun* locus, we conducted FISH analysis of tomato DNA fibers using fluorescently labeled probes derived from the *L. esculentum* clones Le37F23 and Le33O1 that flank *sun* (Figure 2C). As shown in Figure 4, the fiber FISH results pointed to a distance between clones Le37F23 and Le33O1 of 68 kb (±10.9) in Sun-1642 (Figure 4A) and 38 kb (±6.1) in LA1589 (Figure 4B), respectively, and this difference was highly significant (*t*-test, $P < 0.0001$). This result indicated that the genomic region lacking from the large insert libraries was relatively small. Furthermore, the *sun* locus was ~30 kb larger in the *L. esculentum* cv Sun1642 compared to the wild relative, *L. pimpinellifolium* LA1589. Thus, this result suggested that allelic variation at *sun* may be due to an insertion/deletion event in this region of the tomato genome. Although the *L. pennellii* clones Lp81B9 and Lp61O2 mapped closer to *sun*, the occurrence of genome rearrangements in this region of the *L. pennellii* genome (see above) prompted us to conduct fiber FISH analysis with the *L. esculentum* clones instead. In addition, the telomeric origin of the insert of clone Lp81B9 resulted in a highly repetitive hybridization signal, rendering this clone difficult to use for fiber FISH analysis (Figure 3, E and F).

Fiber FISH hybridization signals of probes Le37F23 and Le33O1: Clone Le37F23 is located on the centromeric side of *sun*, and fiber FISH analysis shows that this clone measured 193 kb (±11.7) in Sun1642 and 196 kb (±9.7) in LA1589 (Figure 4, A and B). DNA of clone Le37F23 was also run on a CHEF gel and the insert size of this clone was estimated at 177 kb (data not shown), supporting the results obtained from fiber FISH.

The fiber FISH hybridization signal obtained using clone Le33O1, located on the telomeric side of *sun*, appeared more complicated. Fluorescently labeled Le33O1 probe hybridized to tomato DNA fibers showed a short signal overlapping with and adjacent to the signal of probe Le37F23, a gap, and a larger signal (Figure 4, A and B). The most likely explanation for the short signal from probe Le33O1 overlapping with and adjacent to the signal of probe Le37F23 was that the end of the first contig (contig LPT4D21) proximal to *sun* was repeated in the second contig (Lp81B9-F/Lp103E7-R contig) and that this short signal from Le33O1 merely represented the duplicated segment. This hypothesis was supported by the fact that probes Lp103E7-R and Lp81B9-FF hybridized to clone Le33O1, even though the contigs failed to overlap (Figure 2C). Therefore, it is likely that the larger signal represents the actual length of clone Le33O1 in the Sun1642 and LA1589 genomes. The larger signal measured 38 kb (±8.9) in Sun1642 and 33 kb (±5.8) in LA1589, respectively, and this difference was not significant at the 5% level (*t*-test, $P < 0.07$). CHEF gel analysis of clone Le33O1 indicated that the insert of this clone measured 42 kb (data not shown), consistent with the insert size estimated by fiber FISH analysis to Sun1642 DNA.

Duplication flanking sun: To confirm that *sun* is flanked

by a genome duplication and that the unusual fiber FISH hybridization pattern of Le33O1 is not due to an aberrant and rearranged clone, Southern blot analyses were performed using markers flanking *sun*. The Southern blot contained restriction-enzyme-digested genomic DNA isolated from Sun1642 and LA1589 leaf tissue. The hybridization results with probe Lp81B9-FF showed two characteristic bands for each parent, indicating the duplicated nature of Lp81B9-FF (Table 1 and Figure 5). Hybridizing probe Lp104D16-F, which maps very close to Lp81B9-FF, to the same blot showed only one of the characteristic *Eco*RI and *Sca*I bands for each parent, while probe Le33O1-R, on the other side of the *sun* locus, hybridized to the other *Eco*RI and *Sca*I fragments (Figure 5). Several recombination events separated markers Lp104D16-F and Le33O1-R, which indicated that the two characteristic *Eco*RI and *Sca*I bands were not due to an *Eco*RI or a *Sca*I restriction enzyme site within the RFLP probe. Fiber FISH analysis conducted with *L. pennellii* clone Lp61O2, which overlapped with Le33O1 (Figure 2C), showed a similar fiber FISH pattern as Le33O1 (data not shown). Combined, these results strongly suggest that the disrupted fiber FISH signal of probe Le33O1 is not due to a rearranged clone. Instead these results demonstrate the presence of a duplicated region flanking *sun*.

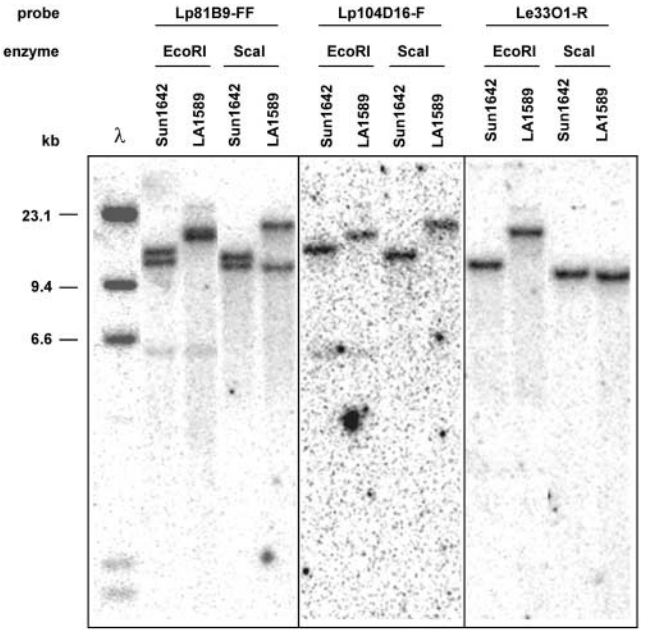

FIGURE 5.—Southern blot analysis with probes derived from genomic DNA fragments flanking *sun*. The left lane depicts the DNA size marker. Southern blot-transferred genomic DNA cut with restriction enzymes indicated above the lane showed hybridization of probe Lp81B9-FF (left) to two restriction fragments in both Sun1642 and LA1589. Probe Lp104D16-F showed hybridization to one of the restriction fragments (middle), while probe Le33O1-R showed hybridization to the other restriction fragment (right).

DISCUSSION

High-resolution recombinant screens demonstrated the precise map location of *sun* to a region on the short arm of chromosome 7 comprising <68 kb. The two recombinant screens combined with cytogenetic, genetic, and Southern blot analyses provided detailed insights into the chromosome structure of this locus. Our results showed that *sun* is located in a region of the tomato genome that appears to be prone to DNA rearrangements. First, the locus experienced an ~30-kb insertion/deletion event. Second, *sun* maps close to an inversion breakpoint that occurred in a distant wild relative, *L. pennellii* accession LA716. Third, the *sun* locus appears to interrupt a tandem duplication.

The size of the *sun* locus measured 38 kb in the wild relative *L. pimpinellifolium* LA1589, while this locus measured 68 kb in the cultivated counterpart *L. esculentum* cv Sun1642. The insertion/deletion may be the cause of allelic variation at this locus. For example, duplication of a gene(s) in Sun1642 may result in higher gene dosage effects in Sun1642 and, hence, increased fruit elongation. Alternatively, deletion of a gene limiting growth may also result in increased fruit elongation. On the other hand, allelic variation may be due to the position effect of the insertion/deletion resulting in disruption or changes in the regulation of the affected gene.

The inversion breakpoint and *sun* are located in close proximity to each other. Allelic variation at *sun* between Sun1642 and LA1589 and between Sun1642 and LA716 resulted in a similar fruit-shape phenotype; *i.e.*, the wild alleles imparted a round-shaped fruit, while the Sun1642 allele imparted an elongated-shaped fruit (Tables 2 and 3). This result indicates that the inversion in *L. pennellii* LA716 *per se* does not affect fruit morphology.

Paracentric inversion in *L. pennellii*: The cosegregation of several markers in the high-resolution recombinant screen of the EPN population, the large genetic distance between the ends of *L. pennellii* clone Lp103E7 in the EPM population (Figure 2A), and the pachytene FISH analysis results provide strong evidence for the presence of an inversion of a portion of the short arm of chromosome 7 in the *L. pennellii* accession LA716 genome compared to Sun1642 and LA1589 genomes. The presence of a chromosome 7 inversion in LA716 was suspected because many markers on the short arm of chromosome 7 cosegregate in the tomato high-density molecular map, which is based on an F_2 population derived from a LA716 and *L. esculentum* cross (PILLEN *et al.* 1996). Instead, populations derived from *L. pimpinellifolium* LA1589 and *L. esculentum* (GRANDILLO and TANKSLEY 1996; this study) and from *L. peruvianum* LA2157 and *L. esculentum* (VAN HEUSDEN *et al.* 1999) show comparable levels of recombination between these markers, indicating absence of a similar inversion in other Lycopersicon species. Other regions of the *L. pennellii* LA716 genome have been suspected to harbor

DNA arrangements as well (Bonnema *et al.* 1997). On the short arm of chromosome 1 near the Cf-4/Cf-9 gene cluster, several markers are found to map together in an F_2 population derived from the LA716 and *L. esculentum* cross. These same markers span a 13-cM region in a population derived from a cross between *L. peruvianum* LA2157 and *L. esculentum* (Bonnema *et al.* 1997).

Like tomato, potato (*S. tuberosum*) and eggplant (*S. melongena*) belong to the Solanum clade within the Solanaceae family (Olmstead and Palmer 1997). The marker order in potato, a very close relative of tomato, appears the same as in the EPM population, given that potato marker CP52 maps toward the telomere and GP121 toward the centromere of potato chromosome 7 (Gebhardt *et al.* 1991). This suggests that the LA716 chromosome 7 inversion is not present in cultivated potato. However, the marker order in eggplant, a more distant relative of tomato and potato, is reversed compared to the marker order in the EPM population, and the breakpoint of the inversion is located to a similar position as in LA716 (Doganlar *et al.* 2002). This would suggest that the inversion in eggplant and *L. pennellii* occurred independently during evolution. The occurrence of independent breakpoints in the near vicinity of each other implies the presence of a genomic region at which chromosomal breakpoints may occur relatively easily.

Recombination frequencies at and near the *sun* locus: Fiber FISH analysis showed that the region encompassing *sun* measures 193 (Le37F23) + 38 (gap) + 33 (Le33O1) = 264 kb. The CHEF gel analysis showed results that are similar to the fiber FISH results; *i.e.*, the *sun* region measures 177 + 38 (gap measured by fiber FISH analysis) + 42 = 257 kb. The 67 recombination events that occurred in this interval indicated an average rate of 1 recombination event/3.8–3.9 kb and a physical-to-genetic distance ratio of 103–106 kb/cM. This physical-to-genetic distance ratio of the *sun* region is well below the genome average of 750 kb/cM (Tanksley *et al.* 1992), but similar to recombination hotspots observed at *I2* on chromosome 11 (43 kb/cM; Segal *et al.* 1992) and at *jointless* on chromosome 11 (<50 kb/cM; Mao *et al.* 2001).

Population-specific differences in recombination frequencies: The genetic distance between markers Le76E24-U and Le124E22-U in the EPN population was 10-fold lower than the genetic distance between these same markers in the EPM population: 0.2 *vs.* 2.3 cM, respectively (Figure 2, B and C). The 10-fold difference in recombination frequency is likely due to the often-observed decrease in recombination frequencies when working with near-isogenic lines such as the EPN population compared to the F_3 lines of the EPM population (Alpert and Tanksley 1996). In addition, decreased frequencies may be due to increased base-pair heterologies between the more distant *L. esculentum* and *L. pennellii* rather than *L. esculentum* and *L. pimpinellifolium* genomes. Similar differences in recombination frequency between different crosses were reported for the nematode resistance gene *Mi-1* (Kaloshian *et al.* 1998). The 550-kb region surrounding *Mi-1* could not be resolved in near-isogenic lines differing for the *Mi-1* allele. However, an intraspecific cross between a susceptible and resistant accession of *L. peruvianum* showed sufficient rates of recombination that allowed map-based cloning of *Mi-1* despite its location near the centromere of chromosome 6 (Kaloshian *et al.* 1998). As in our study, the *Mi-1* fine-mapping results indicate a reduction in recombination frequencies when working with nearly isogenic lines and populations derived from crosses between more distant parents compared to F_2 and F_3 populations derived from closely related parents.

Genome position affects variation in recombination frequency and distribution (Schnable *et al.* 1998). In tomato and other plant species, greatly reduced rates of recombination are observed near and on centromeric regions (Ganal *et al.* 1989; Frary *et al.* 1996; Zhong *et al.* 1999) and in retroelements, transposons, and other highly repetitive regions (Yao *et al.* 2002). It has been shown that gene-rich regions and intergenic regions containing unique DNA generally show several orders of magnitude higher-than-average recombination rates (Faris *et al.* 2000); however, not every gene comprises a recombination hotspot (Yao *et al.* 2002). *sun* is located neither in or near the centromere of tomato chromosome 7, which maps right below CD57 (Figure 2A; Frary *et al.* 1996), nor in the telomere in the Sun1642 and LA1589 genome (Figure 3). Furthermore, *sun* does not appear to be located in a region of highly repetitive DNA, since nearly all clone ends showed unique or two bands on DNA blots (Table 1). Therefore, the results suggest that *sun* is located in a relatively unique region of the tomato genome, which is perhaps gene rich as well.

Unfortunately, we were unable to identify clones spanning this genomic region from several tomato large genomic insert libraries, impeding our progress toward map-based cloning of *SUN*. The libraries screened reportedly cover the genome up to 15 times (Budiman *et al.* 2000). The reason for missing genomic regions in these libraries may be due to reduced efficiency in cloning of certain fragments, the inherent instability of the clone, or the preparation of genomic DNA, *i.e.*, partial *Hin*dIII digestion, prior to ligation of these fragments to the vector. For example, multiple *Hin*dIII sites within a short genomic distance may prevent cloning of contiguous segments of a genome. In addition, we observed that several ends of *L. esculentum* clones identified in the LPT4D21 contig were identical to one another. For example, Le236C15-U was identical to Le27J5-L and Le278H2-L (Figure 2C). Likewise, Le124E22-U was identical to Le278H2-U. These results may suggest *Hin*dIII digestion "hotspots" in the genome. Currently, we are progressing with the map-based cloning of *SUN* via

screening of phage λ genomic libraries (E. van der Knaap and E. Stockinger, unpublished results).

We thank J. J. Giovannoni for the *L. pennellii* large genomic insert libraries, S. Kresovich for the use of the dHPLC, Kai-Yi Chen for clone LPT4D21, the Plant Breeding Department at Cornell for use of equipment, and David Francis and David Mackey for critical reading of this manuscript. This work is supported by an Ohio Agricultural Research and Development Center Seed Grant to E.v.d.K. and the U.S. Department of Agriculture Plant Genome Program (no. 97-35300-4384) and the National Science Foundation (no. DBI-9872617) to S.D.T.

LITERATURE CITED

Alpert, K. B., and S. D. Tanksley, 1996 High-resolution mapping and isolation of a yeast artificial chromosome contig containing fw2.2: a major fruit weight quantitative trait locus in tomato. Proc. Natl. Acad. Sci. USA **93:** 15503–15507.

Bernatzky, R., and S. D. Tanksley, 1986 Towards a saturated linkage map in tomato based on isozymes and random cDNA sequences. Genetics **112:** 887–898.

Bonnema, G., D. Schipper, S. Van Heusden, P. Zabel and P. Lindhout, 1997 Tomato chromosome 1: high resolution genetic and physical mapping of the short arm in an interspecific *Lycopersicon esculentum* × *L. peruvianum* cross. Mol. Gen. Genet. **253:** 455–462.

Budiman, M. A., L. Mao, T. C. Wood and R. A. Wing, 2000 A deep-coverage tomato BAC library and prospects toward development of an STC framework for genome sequencing. Genome Res. **10:** 129–136.

Doganlar, S., A. Frary, M. C. Daunay, R. N. Lester and S. D. Tanksley, 2002 A comparative genetic linkage map of eggplant (*Solanum melongena*) and its implications for genome evolution in the Solanaceae. Genetics **161:** 1697–1711.

Eshed, Y., and D. Zamir, 1994 A genomic library of *Lycopersicon pennellii* in *Lycopersicon esculentum*—a tool for fine mapping of genes. Euphytica **79:** 175–179.

Faris, J. D., K. M. Haen and B. S. Gill, 2000 Saturation mapping of a gene-rich recombination hot spot region in wheat. Genetics **154:** 823–835.

Feinberg, A. P., and B. Vogelstein, 1983 A technique for radiolabeling DNA restriction endonuclease fragments to high specific activity. Anal. Biochem. **132:** 6–13.

Frary, A., G. G. Presting and S. D. Tanksley, 1996 Molecular mapping of the centromeres of tomato chromosomes 7 and 9. Mol. Gen. Genet. **250:** 295–304.

Frary, A., T. C. Nesbitt, A. Frary, S. Grandillo, E. van der Knaap *et al.*, 2000 *fw2.2*: a quantitative trait locus key to the evolution of tomato fruit size. Science **289:** 85–88.

Fridman, E., T. Pleban and D. Zamir, 2000 A recombination hotspot delimits a wild-species quantitative trait locus for tomato sugar content to 484 bp within an invertase gene. Proc. Natl. Acad. Sci. USA **97:** 4718–4723.

Fulton, T. M., J. Chunwongse and S. D. Tanksley, 1995 Microprep protocol for extraction of DNA from tomato and other herbaceous plants. Plant Mol. Biol. Rep. **13:** 207–209.

Ganal, M. W., N. D. Young and S. D. Tanksley, 1989 Pulsed-field gel electrophoresis and physical mapping of large DNA fragments in the *Tm-2a* region of chromosome 9 in tomato. Mol. Gen. Genet. **215:** 395–400.

Gebhardt, C., E. Ritter, A. Barone, T. Debener, B. Walkemeier *et al.*, 1991 RFLP maps of potato and their alignment with the homoeologous tomato genome. Theor. Appl. Genet. **83:** 49–57.

Grandillo, S., and S. D. Tanksley, 1996 QTL analysis of horticultural traits differentiating the cultivated tomato from the closely related species *Lycopersicon pimpinellifolium*. Theor. Appl. Genet. **92:** 935–951.

Grandillo, S., H. M. Ku and S. D. Tanksley, 1999 Identifying the loci responsible for natural variation in fruit size and shape in tomato. Theor. Appl. Genet. **99:** 978–987.

Isaacson, T., G. Ronen, D. Zamir and J. Hirschberg, 2002 Cloning of *tangerine* from tomato reveals a carotenoid isomerase essential for the production of beta-carotene and xanthophylls in plants. Plant Cell **14:** 333–342.

Jackson, S. A., M. L. Wang, H. M. Goodman and J. Jiang, 1998 Application of fiber-FISH in physical mapping of *Arabidopsis thaliana*. Genome **41:** 566–572.

Jiang, J., S. Nasuda, F. Dong, C. W. Scherrer, S. S. Woo *et al.*, 1996 A conserved repetitive DNA element located in the centromeres of cereal chromosomes. Proc. Natl. Acad. Sci. USA **93:** 14210–14213.

Kaloshian, I., J. Yaghoobi, T. Liharska, J. Hontelez, D. Hanson *et al.*, 1998 Genetic and physical localization of the root-knot nematode resistance locus Mi in tomato. Mol. Gen. Genet. **257:** 376–385.

Konieczny, A., and F. M. Ausubel, 1993 A procedure for mapping Arabidopsis mutation using codominant ecotype-specific PCR-based markers. Plant J. **4:** 403–410.

Livingstone, K. D., V. K. Lackney, J. R. Blauth, R. Van Wijk and M. K. Jahn, 1999 Genome mapping in Capsicum and the evolution of genome structure in the Solanaceae. Genetics **161:** 1697–1711.

Mao, L., D. Begum, S. A. Goff and R. A. Wing, 2001 Sequence and analysis of the tomato JOINTLESS locus. Plant Physiol. **126:** 1331–1340.

Olmstead, R. G., and J. D. Palmer, 1997 Implications for the phylogeny, classification, and biogeography of Solanum from cpDNA restriction site variation. Syst. Bot. **22:** 19–29.

Pillen, K., O. Pineda, C. Lewis and S. D. Tanksley, 1996 Status of genome mapping tools in the taxon *Solanaceae*, pp. 281–308 in *Genome Mapping in Plants*, edited by A. Paterson. R. G. Landes, Austin, TX.

Pnueli, L., L. Carmel-Goren, D. Hareven, T. Gutfinger, J. Alvarez *et al.*, 1998 The *SELF-PRUNING* gene of tomato regulates vegetative to reproductive switching of sympodial meristems and is the ortholog of *CEN* and *TFL1*. Development **125:** 1979–1989.

Sambrook, J., E. F. Fritsch and T. Maniatis, 1989 *Molecular Cloning: A Laboratory Manual*. Cold Spring Harbor Laboratory Press, Cold Spring Harbor, NY.

Schnable, P. S., A. P. Hsia and B. J. Nikolau, 1998 Genetic recombination in plants. Curr. Opin. Plant Biol. **1:** 123–129.

Schweizer, G., M. W. Ganal, H. Ninnemann and V. Hemleben, 1988 Species-specific DNA sequences for the identification of somatic hybrids between *Lycopersicon esculentum* and *Solanum acaule*. Theor. Appl. Genet. **75:** 679–684.

Segal, G., M. Sarfatti, M. A. Schaffer, N. Ori, D. Zamir *et al.*, 1992 Correlation of genetic and physical structure in the region surrounding the I2 *Fusarium-oxysporum* resistance locus in tomato. Mol. Gen. Genet. **231:** 179–185.

Tanksley, S. D., M. W. Ganal, J. P. Prince, M. C. De Vincente, M. W. Bonierbale *et al.*, 1992 High-density molecular linkage maps of the tomato and potato genomes. Genetics **132:** 1141–1160.

Underhill, P. A., L. Jin, A. A. Lin, S. Q. Mehdi, T. Jenkins *et al.*, 1997 Detection of numerous Y chromosome biallelic polymorphisms by denaturing high-performance liquid chromatography. Genome Res. **7:** 996–1005.

van der Knaap, E., and S. D. Tanksley, 2001 Identification and characterization of a novel locus controlling early fruit development in tomato. Theor. Appl. Genet. **103:** 353–358.

Van Heusden, A. W., M. Koornneef, R. E. Voorrips, W. Bruggemann, G. Pet *et al.*, 1999 Three QTLs from *Lycopersicon peruvianum* confer a high level of resistance to *Clavibacter michiganensis* ssp. *michiganensis*. Theor. Appl. Genet. **99:** 1068–1074.

Wilson, W. A., S. E. Harrington, W. L. Woodman, M. Lee, M. E. Sorrells *et al.*, 1999 Inferences on the genome structure of progenitor maize through comparative analysis of rice, maize and the domesticated panicoids. Genetics **153:** 453–473.

Yao, H., Q. Zhou, J. Li, H. Smith, M. Yandeau *et al.*, 2002 Molecular characterization of meiotic recombination across the 140-kb multigenic *a1-sh2* interval of maize. Proc. Natl. Acad. Sci. USA **99:** 6157–6162.

Zhong, X., P. F. Fransz, E. J. Van Wennekes, P. Zabel, A. Van Kammen *et al.*, 1996 High-resolution mapping on pachytene chromosomes and extended DNA fibers by fluorescence *in-situ* hybridisation. Plant Mol. Biol. Rep. **14:** 232–242.

Zhong, X., P. F. Fransz, J. Wennekes-Van Eden, M. S. Ramanna, A. Van Kammen *et al.*, 1998 FISH studies reveal the molecular

and chromosomal organization of individual telomere domains in tomato. Plant J. **13:** 507–517.

Zhong, X., J. Bodeau, P. F. Fransz, V. M. Williamson, A. Van Kammen *et al.*, 1999 FISH to meiotic pachytene chromosomes of tomato locates the root-knot nematode resistance gene *Mi-1* and the acid phosphatase gene *Aps-1* near the junction of euchromatin and pericentromeric heterochromatin of chromosomes arms 6S and 6L, respectively. Theor. Appl. Genet. **98:** 365–370.

Communicating editor: B. Bartel